



Effect of the unbonding materials on the mechanic behavior of all-steel buckling-restrained braces



Quan Chen^a, Chun-Lin Wang^{a,*}, Shaoping Meng^a, Bin Zeng^b

^aKey Laboratory of Concrete and Prestressed Concrete Structures of the Ministry of Education, Southeast University, Nanjing 210096, China

^bCentral Research Institute of Building and Construction, MCC Group, Beijing 100088, China

ARTICLE INFO

Article history:

Received 15 June 2015

Revised 15 December 2015

Accepted 17 December 2015

Available online 11 January 2016

Keywords:

All-steel BRBs

Unbonding materials

Compression strength adjustment factor

Friction force

Residual deformation

ABSTRACT

Seven all-steel buckling-restrained braces (BRBs) were tested under cyclic loading to investigate the effect of the unbonding materials on the performance of BRBs, via the employment of a layer of 1-mm thick butyl rubber or pure air gap between the core plate and the restraining system. Test results indicate that all the BRBs exhibited rather well energy dissipation capacities and sustained cumulative plastic deformations over 1000 times the yield strain. However, significantly higher compression strength adjustment factor β was developed for the specimens without the unbonding materials, due to the gradually increasing friction force and the jamming between the end of the core plate and the restraining members. Moreover, the gradually increasing friction force and the jamming also induced the considerably nonuniform residual deformation for the specimens without the unbonding materials both observed in the test and the finite element models. Especially, for high performance BRBs with relatively long yielding segment and thin core plate, the unbonding materials are recommended to apply.

© 2015 Elsevier Ltd. All rights reserved.

1. Introduction

Centrally braced frames have been prevalent owing to their large lateral stiffness with less lateral displacement under severe earthquake at a low cost. However, damages of the braces due to buckling have been frequently found under severe earthquakes (e.g., the 1994 Northridge earthquake [1]), which limited the ductility and energy dissipation capacity of the frames. Alternatively, buckling-restrained braced frames (BRBFs), with both high lateral stiffness and stable hysteretic properties, have been increasingly popular among designers. Buckling-restrained brace (BRB) is a special type of brace with global buckling inhibited by an appropriate restraining system, which implies the compression hysteretic behavior similar to the tension hysteretic behavior.

In the recent decades, a number of studies have been conducted both at the component and frame levels to develop different types of BRBs for seismic hazard mitigation. At the component level, Black et al. [2] experimentally verified the results of theoretical predictions on the structural stability of the braces, and validate the inelastic capacity of the braces under severe earthquake demands. Further, Wang et al. [3] developed a type of aluminum

alloy buckling-restrained braces to enhance the durability of BRBs in bridge engineering. In order to improve the low-cycle fatigue performance of BRBs, Wang et al. [4] employed toe-finished method in the welds between the ribs and the core plate. Besides, Zhao et al. [5] proposed and experimentally validated a global stability design method of BRBs considering the effect of end bending moment transfer. At the frame level, Wu et al. [6] provided design procedures to quantify the responses of BRBFs. In order to investigate the seismic behavior of the proposed BRBs, Tsai et al. [7,8] conducted pseudo-dynamic test on a full-scale 3-story 3-bay BRBF. Moreover, Sabelli et al. [9] and Fahnestock et al. [10] have predicted seismic response requirements for the design of BRBFs through a great amount of numerical analysis. Chen et al. [11] investigated the seismic demand of the BRBs which was employed to retrofit a steel arch bridge under severe earthquake.

Generally, the members used to restrain the buckling of the core plate in conventional BRBs are mortar or concrete cased in a steel tube. Between the core plate and the restraining members, unbonding materials are employed, not only to reduce the adhesion force between the core plate and the restraining members, but to provide the space for the expansion of the core plate under compression. Primarily, Wakabayashi et al. [12] conducted adhesion test on several materials, concluding that a layer of epoxy resin and silicon resin was the preferable unbonding materials. Until now, several unbonding materials (e.g. epoxy resin, silicon resin, vinyl tapes, etc.) have been widely employed in BRBs [13].

* Corresponding author at: School of Civil Engineering, Southeast University, Nanjing 210096, China.

E-mail address: chunlin@seu.edu.cn (C.-L. Wang).

Especially, Tsai et al. [13] tested ten BRBs with different unbonding materials and found that a 2-mm thick silicon rubber sheet had the least axial load difference for the proposed BRB. Moreover, Tsai et al. [14] tested four BRB specimens with different unbonding materials (high density styrofoam sheet, chloroprene rubber, rubber sheet and silicone sheet), and compared their hysteretic properties and cost effect.

However, it is time-consuming to pour and cure the concrete or mortar in conventional BRBs, and local buckling was observed due to the crush of the concrete or mortar in certain experiments [15,16]. Therefore, different types of BRBs with restraining members mainly made of steel, designated as all-steel BRBs, have been proposed by several researchers in the last few years. Since the adhesion between the steel core plate and the steel restraining members is negligible and the space for the expansion of the core plate can be provided by controlling the dimension of the steel restraining members, the unbonding materials seem not indispensable in all-steel BRBs. But several types of lubricant were still employed on the surfaces of the core plate in all-steel BRBs [17,18]. Recently, in the experiment presented in the literature [19], a small air gap was used between the core plate and the steel restraining tubes instead of the unbonding materials, which did not affect the cyclic behavior of the proposed BRB evidently. Della Corte et al. [20] also employed the air gap in all-steel BRBs and controlled the peak compression resistance through appropriate design of casing connections. Contradictory to those, Iwata [21] tested all-steel BRBs without the unbonding materials and found they finally fractured as a result of the continued progress of the plastic deformation. Likewise, Tremblay et al. [22] compared the performance of the conventional BRBs to all-steel BRBs without the unbonding materials, indicating that it is necessary to minimize the friction to develop the uniform strain in the core plate.

Since the role of the unbonding materials in all-steel BRBs is uncertain to date, more research needs to be conducted. In this article, two series of test specimens, comprised of seven all-steel BRB specimens, were designed to estimate the effect of the unbonding materials on the low-cycle fatigue performance of the all-steel BRBs. Different factors, including the existence of the unbonding materials, the testing protocol and the width of the in-plane gap, were employed in the test program for comparison.

2. High-mode buckling of the all-steel BRB

The employed all-steel BRB consists of a steel core plate, a pair of steel restraining plates and a pair of steel fillers, as shown in Fig. 1. Furthermore, the cross-sectional details of the BRB specimens are shown in Fig. 2, where the core plate is inserted between the pair of restraining plates connected by the high-strength bolts through two fillers on both sides of the core plate. Besides, a layer of 1-mm thick butyl sealant tape is adopted between the core plate and the restraining system, while for BRBs without the unbonding

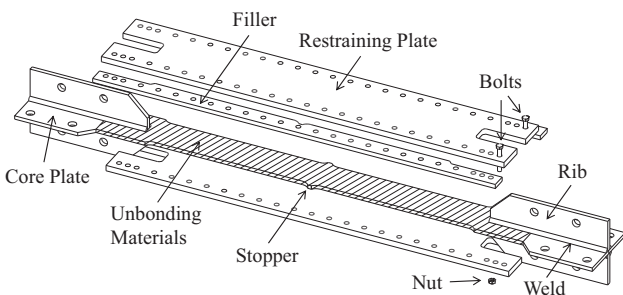


Fig. 1. Assemblage of the all-steel BRB.

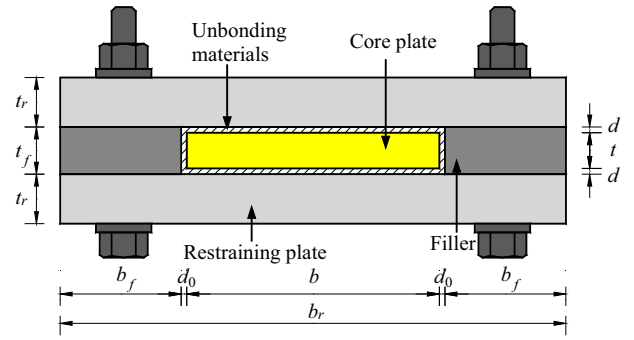


Fig. 2. Cross-sectional details. Note: b_r and t_r are the width and thickness of the restraining plate, respectively; b and t are the width and thickness of the yielding segment, respectively; b_f and t_f are the width and thickness of the fillers, respectively; d_0 and d are the widths of the in-plane and out-of-plane gap between the core plate and the restraining system, respectively.

materials, just 1-mm air gap is alternatively employed. To prevent the slip off the restraining members, the stopper is set at the center via enlarging the width of the core plate.

2.1. Weak-axis high-mode buckling wavelength

Even though global flexural buckling of the BRB under a large compressive strain can be prevented with sufficient stiffness of the restraining members [23], the weak-axis high-mode buckling of the core plate is still inevitable (Fig. 3). Euler formula has been employed to approximate the weak-axis high-mode buckling behavior, using the yield strength and the flexural stiffness of the core plate [19,24]. The buckling wave length was determined by Euler critical load without contact force, but researches have shown that the contact force may increase the critical load [25].

The buckling wave number (n) of a bi-laterally constrained elastic column has been estimated with Eq. (1) by solving the fourth-order, linearized differential equation for an Euler beam under increasing axial compression load [26], where P is the axial load and E is the elastic Young's modulus of the core plate, and L_y is the length of the constrained column (corresponding to the yielding segment of the core plate).

$$1 + 2n \leq \sqrt{\frac{3PL_y^2}{\pi^2 Ebt^3}} \leq 1 + 4n \tag{1}$$

where the left and right sides of the equation correspond to the upper and lower bounds of the number of waves respectively. Since the lateral deflection of the core plate is limited below the out-of-plane gap width ($d = 1$ mm), it is feasible to extend Eq. (1) to the elastic-plastic buckling behavior of the core plate based on the theory of elastic-plastic buckling developed by Shanley [27]. Replacing the Young's modulus E with the tangent modulus E_t in Eq. (1), the weak-axis high-mode buckling wavelength of the core plate l_w can be predicted as follows:

$$\text{int} \left(\frac{1}{2} \sqrt{\frac{3PL_y^2}{\pi^2 E_t bt^3} - \frac{1}{4}} \right) \leq l_w \leq \frac{L_y}{\text{int} \left(\frac{1}{4} \sqrt{\frac{3PL_y^2}{\pi^2 E_t bt^3} - \frac{1}{4}} \right)} \tag{2}$$

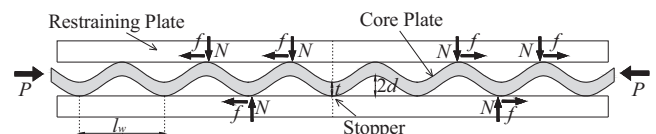


Fig. 3. Weak-axis high-mode buckling of the core plate.

Download English Version:

<https://daneshyari.com/en/article/265884>

Download Persian Version:

<https://daneshyari.com/article/265884>

[Daneshyari.com](https://daneshyari.com)